CHEMISTRY
A EUROPEAN JOURNAL

FULL PAPER

DOI: 10.1002/chem.201302273

Bioconjugation of Proteins with a Paramagnetic NMR and Fluorescent Tag

Feng Huang, Ying-Ying Pei, Hui-Hui Zuo, Jia-Liang Chen, Yin Yang, and Xun-Cheng Su*[a]

Abstract: Site-specific labeling of proteins with lanthanide ions offers great opportunities for investigating the structure, function, and dynamics of proteins by virtue of the unique properties of lanthanides. Lanthanide-tagged proteins can be studied by NMR, X-ray, fluorescence, and EPR spectroscopy. However, the rigidity of a lanthanide tag in labeling of proteins plays a key role in the determination of protein structures and interactions. Pseudocontact shift (PCS) and paramagnetic relaxation enhancement (PRE) are valuable long-range structure restraints in structural-biology NMR spectroscopy. Generation of these paramagnetic restraints generally relies on site-specific tagging of the target proteins with paramagnetic species. To avoid nonspecific interaction between the target protein and paramagnetic tag and achieve reliable paramagnetic effects, the rigidity, stability, and size of lanthanide tag is highly important in paramagnetic labeling of proteins. Here 4′-mercapto-2,2′:6′,2″-terpyridine-6,6″-dicarboxylic acid (4MTDA) is introduced as a a rigid paramagnetic and fluorescent tag which can be site-specifically attached to a protein by formation of a disulfide bond. 4MTDA can be readily immobilized by coordination of the protein side chain to the lanthanide ion. Large PCSs and RDCs were observed for 4MTDA-tagged proteins in complexes with paramagnetic lanthanide ions. At an excitation wavelength of 340 nm, the complex formed by protein–4MTDA and Tb^{3+} produces high fluorescence with the main emission at 545 nm. These interesting features of 4MTDA make it a very promising tag that can be exploited in NMR, fluorescence, and EPR spectroscopic studies on protein structure, interaction, and dynamics.

Keywords: fluorescence · lanthanides · NMR spectroscopy · N,O ligands · proteins

Introduction

Tagging proteins with lanthanide ions offers great opportunities for studying biological structures by means of X-ray, NMR, and fluorescence spectroscopy.[1] Lanthanide-tagged proteins have attracted great interest in paramagnetic NMR spectroscopy, because the dipolar interaction of unpaired electron and nuclear spins of proteins are rich sources of structural restraints.[1] These paramagnetic effects on proteins usually include paramagnetic relaxation enhancement (PRE), pseudocontact shift (PCS), and residual dipolar coupling (RDC).[1a] Since most proteins have no natural binding site for paramagnetic ions, generation of these paramagnetic restraints generally relies on site-specific labeling of proteins with paramagnetic tags.[2a–c] However, the flexibility of the paramagnetic tag compromises the quality and accuracy of the three-dimensional structures determined by paramagnetic NMR spectroscopy, because the mobility of the tag enlarges the region of the paramagnetic center relative to the protein surface and hence averages the paramagnetic effects.[2d] Immobilizing the paramagnetic tag is thus a key issue in site-specific labeling of proteins.[2b,d] Several successful strategies have been proposed for restriction of paramagnetic tags, including increasing the size of the tag,[3] the double-point ligation method,[3b,4] anchoring the tag by coordination of a protein,[5] and preventing rotamer transitions of a tag.[5c,6]

The DOTA-like paramagnetic tags and lanthanide-binding peptides usually generate large paramagnetic effects,[3] but they are bulky and their molecular weights are generally greater than 600 Da. 4-Methylmercapto dipicolinic acid (4MMDPA),[5a] 3-mercapto dipicolinic acid (3MDPA),[5b] and 4-mercapto dipicolinic acid (4MDPA)[5c] are small but rigid paramagnetic lanthanide tags; however, they only have three coordinating atoms. As lanthanide ions usually have high coordination numbers (usually 8 or 9),[7] sufficient coordination numbers are desirable in the design of lanthanide-binding tags. Therefore, increasing the number of coordination sites and minimizing the size of lanthanide tags are still challenging in tagging proteins with lanthanide ions.

Moreover, lanthanide complexes have unique photophysical properties that are widely used in biomedical analysis,[1e,8a] and tagging a protein with a luminescent lanthanide complex is a valuable tool in studies on the functions and dynamics of proteins.[1e,8b] Attachment of a fluorescent

[a] F. Huang,[+] Y.-Y. Pei,[+] H.-H. Zuo, J.-L. Chen, Y. Yang, Prof. X.-C. Su
State Key Laboratory of Elemento-organic Chemistry
and College of Chemistry, Nankai University
Weijin Road 94, Tianjin 300071 (P. R. China)
Fax: (+86) 22-23500623
E-mail: xunchengsu@nankai.edu.cn

[+] These authors contributed equally to this work.

Supporting information for this article is available on the WWW under http://dx.doi.org/10.1002/chem.201302273.

tag to a protein proceeds by a similar chemical reaction to paramagnetic labeling of proteins. However, the linker between protein and fluorescent tag is usually long (>10 Å) and flexible, which greatly decreases the precision of the distance between two fluorophores during protein interactions.[9] Site-specific labeling of proteins with a rigid and small tag can therefore improve the interpretation of measured results both in paramagnetic NMR and fluorescence studies on proteins.

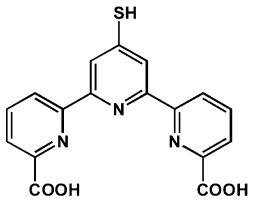

Figure 1. Structure of 4MTDA.

2,2′:6′,2″-Terpyridine and its derivatives are well-known metal-binding ligands.[10] The lanthanide complexes of terpyridine derivatives have been used as fluorescence probes or tags.[11] Herein, we synthesized 4′-mercapto-2,2′:6′,2″-terpyridine-6,6″-dicarboxylic acid (4MTDA, Figure 1) and attached it to human ubiquitin mutants by formation of a disulfide bond.[12]

The molecular weight of 4MTDA of 353 Da is lower than those of commonly used lanthanide-binding peptides and DOTA-like tags[3] (Supporting Information, Figure S1). To explore the rigidity and stability of the 4MTDA tag, two cysteine mutants of human ubiquitin, T22C and A28C, were made and subsequently derivatized with 4MTDA. Significant pseudocontact shifts (PCSs) and residual dipolar couplings (RDCs) were observed in the 4MDTA-tagged proteins in complexes with paramagnetic ions. Interestingly, the lanthanide complex showed no heterogeneity in the protein samples, since no diastereomers were observed in the ^{15}N HSQC spectra. More importantly, the paramagnetic ion is immobilized by the five coordinating atoms of 4MTDA and one carboxylate side chain of an acidic amino acid in a protein. In comparison with the published lanthanide tags, 4MTDA has several advantages: 1) 4MTDA is small and rigid; 2) 4MTDA-tagged proteins can be studied both by NMR and by fluorescence spectroscopy. These interesting features make 4MTDA a very promising lanthanide tag in studies on the structures, interactions, and dynamics of proteins and protein complexes by NMR and fluorescence spectroscopy.

Results

Synthesis of 4MTDA: The synthesis of the 4MTDA is depicted in Scheme 1. Starting from commercially available dipicolinic acid, compound **5** was synthesized according to a previous report.[13] The corresponding thiouronium bromide **6** was obtained from **5** and thiourea in refluxing acetone, similar to the published protocol.[14] The final product 4MTDA was obtained by hydrolysis of **6** in methanol/water.

Interaction of 4MTDA with paramagnetic metal ions: NMR spectroscopy was used to explore the stoichiometry and stability of the complexes formed by 4MTDA and lanthanide ions in aqueous solution. Addition of paramagnetic Nd^{3+} to a solution of 4MTDA in D_2O at pD 7.0 produced a new set of signals indicating slow exchange between free ligand and metal complex. Four sets of resonances were observed for the complex $[Nd(4MTDA)_2]^-$. With increasing concentration of Nd^{3+}, four new peaks corresponding to $[Nd(4MTDA]^+$ were generated. Interestingly, at a $[Nd^{3+}]$/[4MTDA] molar ratio of about 0.44, a large amount of $[Nd(4MTDA]^+$ coexists with $[Nd(4MTDA)_2]^-$ (Figure 2). Addition of Yb^{3+} to a solution of 4MTDA resulted in opposite chemical shifts in comparison with Nd^{3+}. Slow exchange between free ligand, $[Yb(4MTDA)_2]^-$, and $[Yb(4MTDA)]^+$ was also observed (Figure 3). These interesting results indicate that lanthanides bind the first 4MTDA ligand more tightly than additional 4MTDA in the formation of $[Ln(4MTDPA)_2]^-$ complexes.

Accurate binding constants of 4MTDA and lanthanide ions were not determined by NMR spectroscopy due to slow exchange between the free ligand and its metal com-

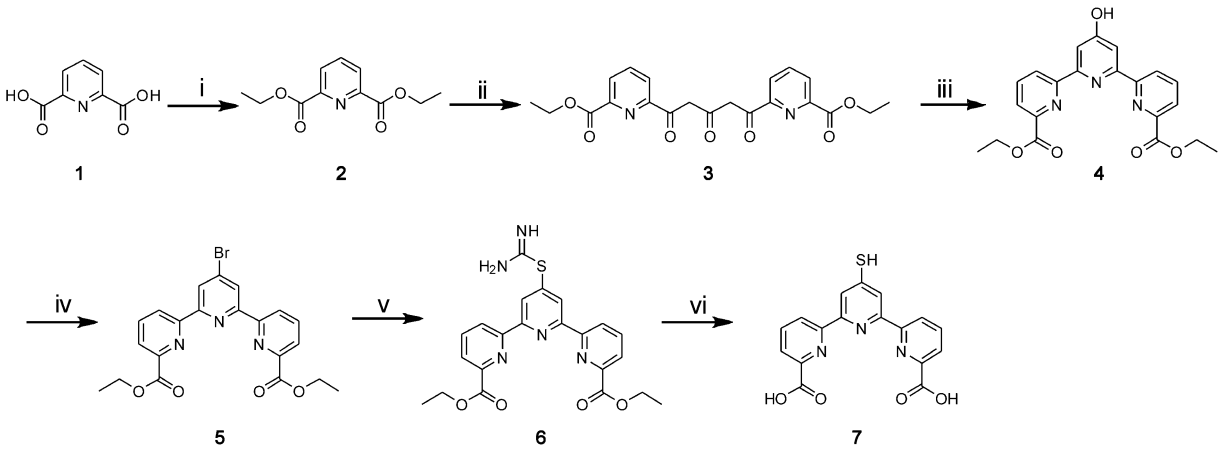

Scheme 1. Synthesis of 4MTDA. i) $SOCl_2$/EtOH; ii) acetone, NaH, THF, 40-45°C; iii) NH_4OAc/EtOH/rf; iv) PBr_3/DMF/Ar/60°C; v) thiourea/acetone/rf; vi) 1) NaOH/MeOH, 2) HCl/H_2O.

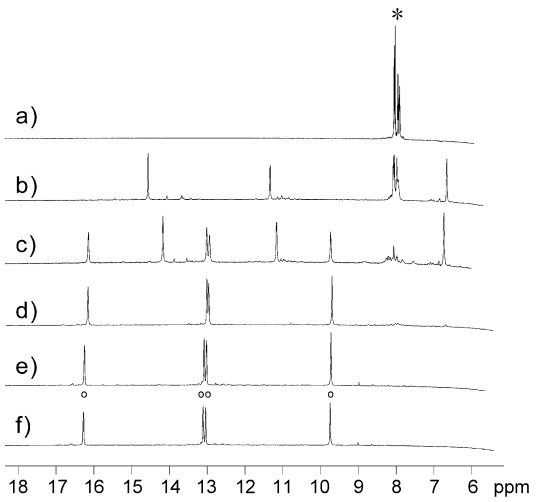

Figure 2. Interaction of 4MTDA with Nd^{3+} determined by NMR spectroscopy. A 10 mM aqueous solution of $NdCl_3$ was titrated into a mixture of 0.8 mM 4MTDA and 2.0 mM dithiothreitol (DTT) in D_2O at pD 7.0. The NMR spectra were recorded at a proton frequency of 600 MHz with increasing $NdCl_3$ concentration: a) 0, b) 0.18, c) 0.35, d) 0.53, e) 0.88, and f) 1.2 mM $NdCl_3$. The asterisk indicates signals of free 4MTDA, and circles indicate those of $[Nd(4MTDA)]^+$.

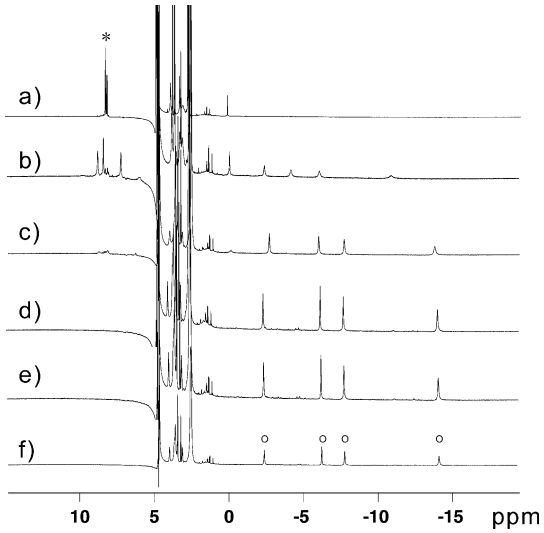

Figure 3. Interaction of 4MTDA with Yb^{3+} determined by NMR spectroscopy. NMR conditions were the same as in Figure 2. a) 0, b) 0.18, c) 0.35, d) 0.53, e) 0.88, and f) 1.2 mM $YbCl_3$. The asterisk indicates the signals of free 4MTDA, and circles indicate those of $[Yb(4MTDA)]^+$.

plexes. Isothermal titration calorimetry (ITC) was carried out to determine the association constants of 4MTDA and lanthanides. At 286 K and pH 6.4 in 20 mM 2-(*N*-morpholino)ethanesulfonic acid (MES) buffer, association constants of Lu^{3+} for the first and second 4MTDA ligands of $(1.4\pm0.2)\times10^7\,M^{-1}$ and $(2.5\pm0.2)\times10^6\,M^{-1}$ were determined, respectively (Supporting Information, Figure S2).

Ligation of proteins with 4MTDA: Chemical modification of proteins with 4MTDA was carried out similarly to the previously established protocol.[12] Since the sulfhydryl group of 4MTDA has a lower pK_a value than 4MMDPA, 4MTDA is less reactive than the published lanthanide binding tag (LBT)[3a,4b,12] and DPA tags.[5] Therefore, eight equivalents of 4MTDA were necessary to give a reasonable amount of protein–4MTDA adducts. The general ligation yield is about 50–70%, and it is lower than that of 4MMDPA, LBT, and 3MDPA.

Stability of protein–4MTDA and lanthanide complexes: To evaluate the thermodynamic stability of 4MTDA-tagged proteins and lanthanide complexes, we titrated dipicolinic acid (DPA) into a mixture of ubiquitin–4MTDA and lanthanide ions. Addition of 0.12 mM DPA to a solution of 0.1 mM ubiquitin A28C–4MTDA and 0.12 mM Tm^{3+} at pH 6.4 had a negligible effect on the ^{15}N HSQC spectrum of the protein sample. The paramagnetic species corresponding to the ubiquitin–4MTDA–Tm complex remained essentially unchanged. When 0.20 mM DPA was added, the paramagnetic species only decreased by 20% in peak intensity. A few peaks showed obvious chemical-shift changes and decreased peak intensity, which probably stem from noncovalent interaction of $[Tm(DPA)_3]^{3-}$ and the protein.[15] This competition experiment suggests that 4MTDA-tagged protein forms highly stable lanthanide complexes in aqueous solution (Supporting Information, Figure S3).

Resonance assignments of the protein–4MTDA adducts: The NMR resonances of protein backbone amido groups were assigned on the basis of 3D ^{15}N NOESY-HSQC and ^{15}N HSQC spectra. Both protein constructs show high-quality NMR spectra. In comparison with the underivatized protein, the chemical-shift changes in ubiquitin–4MTDA constructs were limited to the amido groups in the vicinity of T22C and A28C (Figure 4). The magnitudes of the chemical-shift changes were small and most changes were within 0.10 ppm. The secondary structural segments were retained according to a comparison of NOESY-HSQC and protein

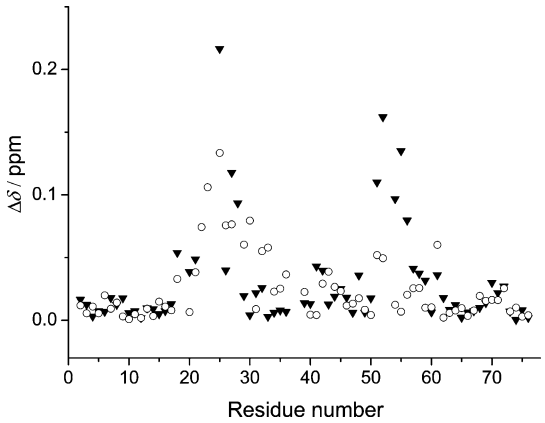

Figure 4. Chemical-shift differences between ubiquitin and ubiquitin–4MTDA. The chemical shifts were calculated as $\Delta\delta=[(\Delta\delta_H)^2+(\Delta\delta_N/10)^2]^{1/2}$. Triangles: T22C and T22C–4MTDA; circles: A28C and A28C–4MTDA.

structure in both protein–4MTDA samples, which suggests that the introduction of 4MTDA causes negligible changes in protein structure.

PCS measurements and $\Delta\chi$ tensors: Significant chemical-shift changes were observed on addition of paramagnetic Dy^{3+}, Tb^{3+}, Tm^{3+}, or Yb^{3+} to a solution of ^{15}N-ubiquitin-4MTDA (Figure 5 and Supporting Information, Figures S4 and S5). All of the paramagnetic metal ions resulted in high-quality NMR spectra. For each backbone amido group, a single cross-peak was observed in the presence of diamagnetic Y^{3+} or any of the paramagnetic ions. No heterogeneity of conformational exchange in the lanthanide-loaded protein samples was determined.

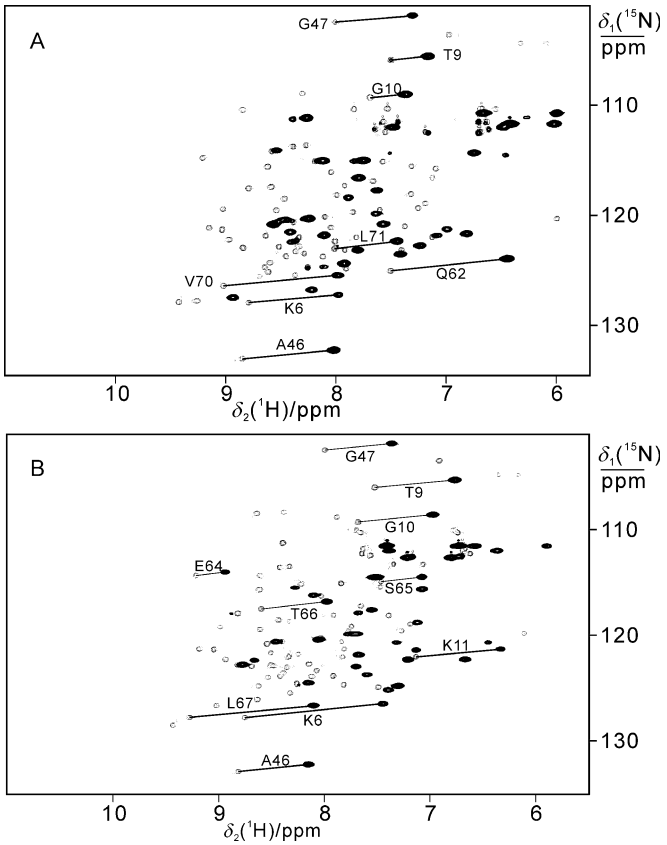

Figure 5. A) Superposition of ^{15}N HSQC spectra of 0.10 mM uniformly ^{15}N labeled T22C–4MTDA in the absence (gray) and presence of 0.10 mM Tb^{3+} (black). B) Superposition of ^{15}N HSQC spectra of 0.1 mM uniformly ^{15}N labeled A28C–4MTDA in the absence (gray) and presence of 0.10 mM Tb^{3+} (black).

The lanthanide-bound and free protein samples show slow exchange, as shown by ^{15}N HSQC spectra. ^{15}N-HSQC spectra were recorded for the complexes of ubiquitin T22C–4MTDA and A28C–4MTDA with Dy^{3+}, Tb^{3+}, Tm^{3+}, and Yb^{3+}, by using the complex with Y^{3+} as the diamagnetic reference. The assignment of the paramagnetic signals was assisted by the fact that the proton and nitrogen spins of a backbone amido group have similar PCSs, because their coordinates differ very little compared to the distance from the paramagnetic center. The paramagnetic cross-peaks are thus displaced along approximately parallel lines from their diamagnetic partner. The PCSs were calculated as chemical shifts of the backbone amide protons in the paramagnetic samples minus those of diamagnetic sample.

Determination of $\Delta\chi$ tensors: The PCSs measured for the ubiquitin–4MTDA complexes with Tb^{3+}, Dy^{3+}, Tm^{3+}, and Yb^{3+} were used to determine the paramagnetic $\Delta\chi$ tensors. Four data sets of PCSs for the residues in well-structured regions were applied in simultaneous fit of the paramagnetic tensors to the crystal structure of ubiquitin. The calculated $\Delta\chi$-tensor parameters are listed in Table 1. The NMR structure was used to evaluate the tensor calculation by using the same PCSs data, and it gave very similar results. Notably, PCSs including those of unstructured residues lead to larger calculated paramagnetic tensors.

Table 1. $\Delta\chi$-tensor parameters [10^{-32} m^3] of ubiquitin–4MDTA complexed with Dy^{3+}, Tb^{3+}, Tm^{3+}, and Yb^{3+}.

		$\Delta\chi_{ax}$	$\Delta\chi_{rh}$	α	β	γ
T22C	Dy^{3+}	31.6	19.3	50.72	144.8	24.0
	Tb^{3+}	30.1	14.0	51.2	149.3	167.6
	Tm^{3+}	−13.6	−8.3	56.7	157.8	168.4
	Yb^{3+}	5.4	3.1	117.7	76.5	62.7
A28C	Dy^{3+}	38.9	5.2	46.2	41.2	17.0
	Tb^{3+}	23.9	15.2	38.1	38.5	174.0
	Tm^{3+}	−12.4	−5.5	37.5	54.3	168.8
	Yb^{3+}	−5.6	−1.6	46.2	47.8	12.1

To verify the calculated $\Delta\chi$ tensors, Figure 6 depicts a plot of experimental and calculated PCS. Excellent correlations between the experimental and calculated data and very small Q factors suggest that the calculated paramagnetic tensors are of high quality.

RDC measurements and calculation of alignment tensors: Significant PCSs observed for the lanthanide-loaded ubiquitin–4MTDA protein samples suggest measurable RDCs, since the anisotropic magnetic susceptibility tensor induces partial alignment of lanthanide-bound proteins. The RDCs for the lanthanide-loaded ubiquitin–4MTDA adducts were measured by comparison of the one-bond ^{1}H–^{15}N splitting observed with paramagnetic lanthanides and diamagnetic Y^{3+}. At 298 K, HN–N RDCs of up to 13 Hz were determined for the Dy^{3+}-loaded protein sample at a magnetic field of 14.1 T. The axial and rhombic components of the alignment tensors were determined by fitting the H–N RDCs of residues in the well-structured regions to the crystal structure of ubiquitin (Table 2). Figure 7 shows the correlations between the experimental and back-calculated RDCs. Larger Q factors than those of PCSs were obtained.

Fluorescence measurements on the ubiquitin–4MTDA adduct in complex with Tb^{3+}: The emission and excitation

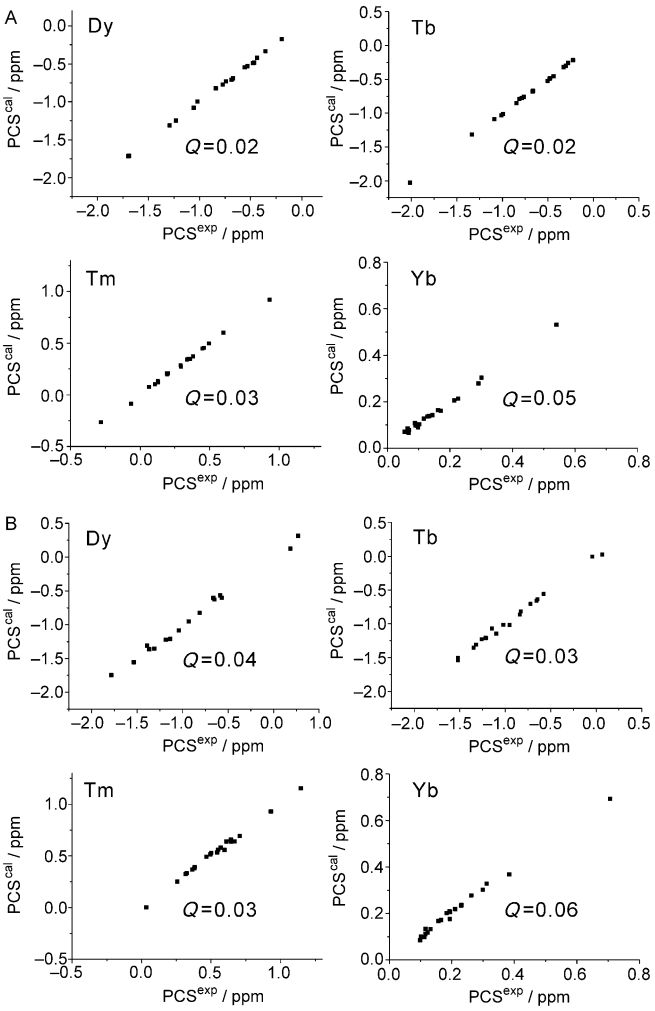

Figure 6. Correlations of the back-calculated PCS (PCS^{cal}) plotted against the experimentally measured PCS (PCS^{exp}) for the complex of 0.10 mM ubiquitin–4MTDA and paramagnetic lanthanide ions, as well as Q factors. A) T22C–4MTDA. B) A28C–4MTDA.

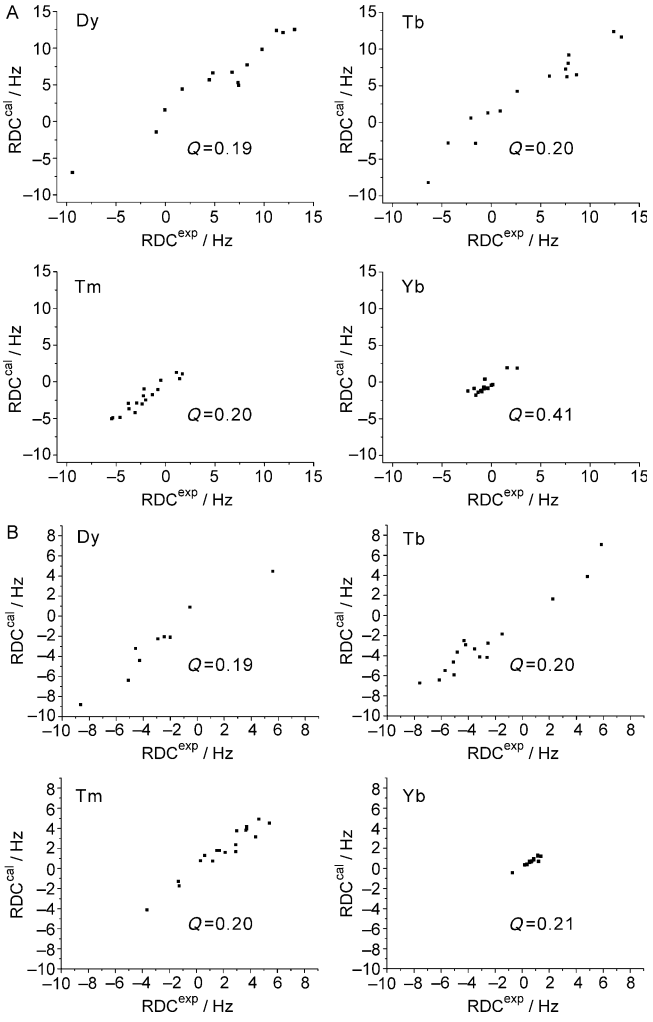

Figure 7. Correlations of the back-calculated RDC (RDC^{cal}) plotted against the experimentally measured RDC (RDC^{exp}) for the complex of 0.10 mM ubiquitin–4MTDA and paramagnetic lanthanide ions, as well as Q factor. A) T22C–4MTDA. B) A28C–4MTDA.

Table 2. Comparison of alignment tensors obtained by RDC fitting and back-calculated from $\Delta\chi$ tensors of ubiquitin–4MTDA complexed with Dy^{3+}, Tb^{3+}, Tm^{3+}, and Yb^{3+}.[a]

	Ln^{3+}	$10^4 A_{ax}$[b]	$10^4 A_{rh}$[b]	$10^4 A_{ax}$[c]	$10^4 A_{rh}$[c]
T22C	Dy^{3+}	5.7	1.9	8.1	4.9
	Tb^{3+}	5.5	1.5	7.7	3.6
	Tm^{3+}	−2.3	−0.9	3.5	2.1
	Yb^{3+}	1.3	0.2	1.4	0.8
A28C	Dy^{3+}	6.5	3.1	9.9	1.3
	Tb^{3+}	5.1	1.1	6.1	3.9
	Tm^{3+}	−3.1	−1.0	3.2	1.4
	Yb^{3+}	−1.0	−0.3	1.4	0.4

[a] All data recorded at 25 °C and 600 MHz ^{1}H NMR frequency. The tensor parameters were obtained by fitting the experimental data to the crystal structure of ubiquitin. [b] Alignment tensor determined with Module program. [c] A_{ax} and A_{rh} back-calculated from the $\Delta\chi$ tensors in Table 1 by using Equation (2).

spectra of the 4MTDA-tagged protein in complex with Tb^{3+} are presented in Figure 8. The Tb^{3+} complexes with ubiquitin–4MTDA shows emission mainly at 545 nm but with different intensity.

Discussion

Interaction of 4MTDA with paramagnetic lanthanide ions: 2,2′:6′,2″-Terpyridine-6,6″-dicarboxylic acid (TDA) and its derivatives are excellent lanthanide chelators which have been widely used in photophysical chemistry.[11a,b,f] However, the thermodynamic stability of the complexes formed by TDA and lanthanide ions has rarely been explored in aqueous solution. The binding constants determined by ITC for the complexes $[Lu(TDA)]^+$ and $[Lu(TDA)_2]^-$ are $(1.4\pm0.2)\times10^7\,M^{-1}$ and $(3.5\pm0.4)\times10^{13}\,M^{-2}$, respectively. They are consistent with a recent report that showed that TDA forms stable complexes with lanthanide ions in methanol.[11f]

Lanthanide ions bind the first DPA molecule with a high association affinity.[16] To further compare the binding affini-

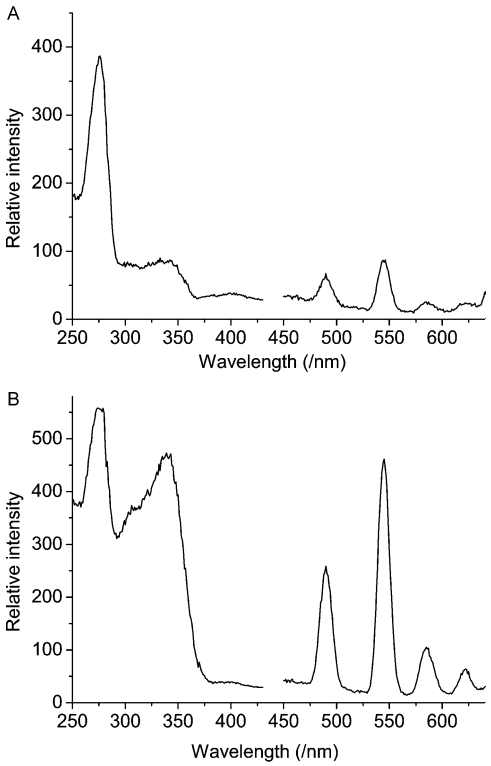

Figure 8. Emission (right) and excitation (left) spectra of 0.05 mM 4MTDA-tagged ubiquitin in complex with 0.06 mM Tb^{3+} in 20 mM MES at pH 6.4 and 298 K; the wavelengths of the excitation and emission spectra are 350 and 545 nm, respectively. A) T22C–4MTDA; B) A28C–4MTDA.

ty of 4MTDA and DPA for lanthanide ions, Figure S6 (Supporting Information) depicts a ^{1}H NMR titration competition experiment in which DPA was titrated into a mixture of Yb^{3+} and 4MTDA. At [DPA]/[4MTDA] = 1.3/1, the abundance of $[Yb(4MTDA)]^+$ is higher than those of $[Yb(DPA)_2]^-$ and $[Yb(DPA)_3]^{3-}$, and the peak intensity of $[Yb(4MTDA)]^+$ remains about 72% of that in the absence of DPA. The competition experiment suggests that 4MTDA has higher binding affinity for lanthanides than DPA.

In comparison with DPA, 4MTDA forms more dynamically stable complexes with lanthanide ions, as determined by 2D H–H exchange spectroscopy (EXSY). At 298 K and pH 7.0, no chemical exchange was observed between $[Y(4MTDA)]^+$ and $[Yb(4MTDA)]^+$ for mixing times of up to 150 ms (data not shown) in a mixture of 1.0 mM 4MTDA, 0.6 mM YCl_3, and 0.8 mM $YbCl_3$. In contrast, significant chemical exchange was determined for a mixture of $[Y(DPA)]^+$ and $[Yb(DPA)]^+$ even when a mixing time of 5 ms was used. This interesting observation is probably due to slow conformational exchange of nonplanar 4MTDA on coordination to lanthanide ions. The dynamic stability of 4MTDA and the lanthanide complexes offers advantages in site-specific labeling of proteins, because chemical exchange between ligand and metal ion averages the paramagnetic effects.

Ligation of proteins with 4MTDA: The lower yield of 4MTDA-tagged protein is probably due to the tautomeric equilibrium between the sulfhydryl and thioketo forms of 4MTDA.[5c] In addition, the solvent susceptibility of cysteine also affects the ligation yield since the less solvent exposed A28C gives a lower yield of 4MTDA derivative than T22C.

PCS measurements and $\Delta\chi$-tensor determination: The paramagnetic ions in complexes with 4MTDA-tagged protein produce very large PCSs, as shown in Figure 5, which indicate that the lanthanide ions are strictly immobilized in the protein complexes. As a consequence, the calculated $\Delta\chi$ tensors of T22C–4MTDA and A28C–4MTDA adducts were similar. The determined paramagnetic tensors are significantly larger than those observed for DPA-tagged proteins.[5] Figure 9 shows the calculated position of the paramagnetic

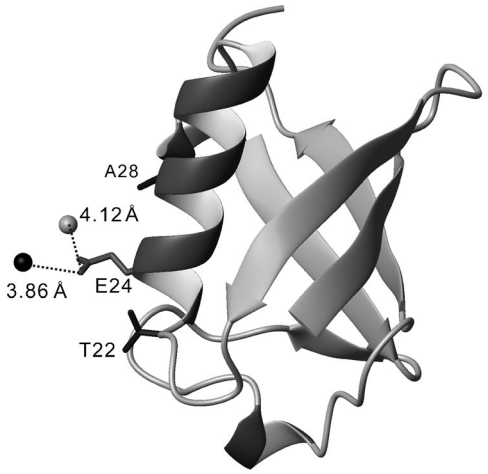

Figure 9. Structural representation of ubiquitin–4MTDA. The calculated paramagnetic centers are shown as black and gray spheres for T22C–4MTDA and A28C–4MTDA, respectively. The calculated distance between the metal ion and the oxygen atom of the E24 side chain is shown.

center with respect to the structure of the protein, and distances of 3.86 and 4.16 Å in Fig. 9, between the metal position and the oxygen atom of E24 side chain were calculated in the T22C–4MTDA and A28C–4MTDA adducts, respectively. Evidently, the carboxylate group of the E24 side chain is coordinated to the lanthanide ion in both protein adducts, in consistence with the calculated large paramagnetic tensors. In the A28C–4MTDA adduct, residue A28 sits in an α helix and residue E24 is located at the i−4 position of the same helix. This in agreement with a recent report that the i and i−4/i+4 positions in an α helix are suitable to anchor a paramagnetic tag by coordination of the protein.[17] In the T22C–4MTDA adduct, the paramagnetic tag is also rigid, despite T22C being located in a loop just before an α helix. This suggests that the distance and orientation between the ligation site and the acidic side-chain residues are favorable for cooperative restriction of lanthanide ions. In both 4MTDA-derivatized T22C and A28C adducts, the distance between the β-carbon atom of each two residues and

the oxygen atom of the E24 side chain is in the range of 6–8 Å, which can be considered a favorable distance for the design of a suitable cysteine mutation based on protein structure.

In the DPA-tagged protein adducts, lanthanide ions are usually fourfold coordinated by three sites of the DPA tag and one of a protein, and the remaining four to five coordination sites are generally occupied by water molecules. In ubiquitin–4MTDA, the lanthanide ion is chelated by 4MTDA and one carboxylate group of the E24 side chain, and two or three water molecules are engaged in the first coordination sphere. This structural feature of 4MTDA-tagged protein and lanthanide ion results in a thermodynamically stable but kinetically inert complex, and thus represents a great advantage in retaining the paramagnetic effects on proteins.

RDC measurements and assessment of 4MTDA rigidity: Anisotropic paramagnetism partially aligns the molecules in an external magnetic field. Sizable RDCs were determined for the lanthanide complexes of 4MTDA-tagged ubiquitin at a proton frequency of 600 MHz (Table 2). In the sample of protein loaded with paramagnetic ions, the correlation between the alignment tensor determined from RDCs and the $\Delta\chi$ tensor determined from PCSs is valuable to assess the mobility of the tag. In general, the PCS is written as Equation (1)[1a]

$$\mathrm{PCS} = \frac{1}{12\pi r^3}[\Delta\chi_{\mathrm{ax}}(3\cos^2\theta - 1) + 1.5\Delta\chi_{\mathrm{rh}}\sin^2\theta\cos 2\phi] \qquad (1)$$

where r, θ, and ϕ are the polar coordinates of the nuclear spin relative to the principal axes of the $\Delta\chi$ tensor and $\Delta\chi_{\mathrm{ax}}$ and $\Delta\chi_{\mathrm{rh}}$ the axial and rhombic components of the $\Delta\chi$ tensor. In a paramagnetically loaded sample, interconversion between the $\Delta\chi$ tensor ($\Delta\chi_{\mathrm{ax,rh}}$) and alignment tensor ($A_{\mathrm{ax,rh}}$) can be written as Equation (2)[1a,5a]

$$A_{\mathrm{ax,rh}} = \frac{B_0^2}{15kT\mu_0}\Delta\chi_{\mathrm{ax,rh}} \qquad (2)$$

where B_0 is the magnetic field strength, μ_0 the induction constant, k the Boltzmann constant, and T the temperature. The PCS can be precisely determined by means of the chemical-shift differences between the paramagnetic and diamagnetic protein samples. However, in a given complex formed by protein and paramagnetic lanthanide ion, the $\Delta\chi$ tensor calculated by PCS increases with increasing distance between the nucleus and the paramagnetic metal ion. The accurate position of the paramagnetic metal ion is therefore important in evaluating the quality of simulated paramagnetic tensors. In Table 2, the alignment tensors determined from RDCs are close to those back-calculated from $\Delta\chi$ tensors, and this suggests that 4MTDA is rigid in the ubiquitin–4MTDA construct complexed with lanthanide ions. Generally smaller RDC-determined alignment tensors compared to the PCS-back-calculated ones are observed in a number of rigid protein–tag constructs.[3abc,5] This observation may also suggest different sensitivity of PCSs and RDCs to protein mobility.[18] This observation can also be justified by comparison of Q factors, as shown in Figures 5 and 6, in which PCS fitting gives much lower Q values.

Fluorescence of ubiquitin–4MTDA in complex with lanthanide ions: The long-lived luminescence of Tb^{3+} and Eu^{3+} complexes has advantages in distance measurements on biomolecules by FRET[19] and also biomedical imaging and analysis.[20] The complex of protein–4MTDA and lanthanide ions is a rigid construct according PCS and RDCs analysis. In comparison with published luminescent lanthanide complexes,[9a,b,11c,d,21] 4MTDA is smaller and more rigid. The luminescent Tb^{3+} complex of A28C–4MTDA shows higher intensity than that of T22C–4MTDA, even though both complexes show the main emission at 545 nm. This is probably due to the mobility of the ligation site in the protein, which may influence the fluorescence of the Tb^{3+} complex.

Conclusion

We have shown that 4MTDA can be ligated to a cysteine residue at position i of an α helix and can be easily immobilized by an aspartate or glutamate residue located in the i−4 or i+4 position, as previously demonstrated.[17] For a protein with known structure, the ligation site can be selected on the basis of a distance of about 6–8 Å between the β-carbon atom of the cysteine residue to be mutated and the nearest oxygen atom of an acidic residue (glutamate or aspartate) side chain. 4MTDA is a small and rigid lanthanide binding tag for site-specific labeling of proteins for structure determination and studies on protein interactions by NMR and fluorescence spectroscopy[1,8,19,20,22] The rigid 4MTDA tag can also be used in high-precision distance measurements on proteins by EPR spectroscopy.[23]

Experimental Section

Synthesis of 4MTDA: Starting from commercial material DPA (**1**), compounds **2**–**5** were obtained by following the published protocols.[13]

Synthesis of 6: Acetone (3.0 mL) was added to a mixture of compound **5** (115 mg, 0.25 mmol) and thiourea (27 mg, 0.36 mmol). The mixture was heated to reflux for 16 h. On cooling, the precipitated white solid was collected by filtration and washed with acetone. The crude produce was dried under reduced pressure (98.0 mg, 86.9%). ^{1}H NMR (400 MHz, [D$_6$]DMSO): δ = 9.39 (s, 3H), 8.93 (d, J = 7.6 Hz, 2H), 8.59 (d, J = 14.7 Hz, 2H), 8.38–8.11 (m, 4H), 4.45 (q, J = 7.0 Hz, 4H), 1.41 ppm (t, J = 7.0 Hz, 6H); ^{13}C NMR (101 MHz, [D$_6$]DMSO): δ = 167.24, 164.29, 155.45, 153.90, 147.58, 139.33, 138.03, 125.98, 125.90, 124.45, 61.50, 14.17 ppm.

Synthesis of 4MTDA (7): Sodium hydroxide solution (1.0 mL, 2.4 mmol) was added dropwise to the suspension of compound **6** (110.0 mg, 0.24 mmol) in 5 mL of methanol under argon protection. The resulting solution was stirred for 3 h and then the pH was adjusted to 2 with 6 M HCl. The orange precipitate was filtered off, washed with cold water, and dried under reduced precessure (80.0 mg, 94.4%). ^{1}H NMR (400 MHz,

D_2O, pD 10): $\delta = 8.19$ (d, $J = 7.9$ Hz, 1H), 8.11 (s, 1H), 8.01 (t, $J = 7.8$ Hz, 1H), 7.92 ppm (d, $J = 7.7$ Hz, 1H).

Expression and purification of protein: Human ubiquitin T22C and A28C mutants were prepared in M9 medium containing $^{15}NHCl_4$ (Isotec) as the sole nitrogen source. The mutant ubiquitin was purified from the soluble fraction of the lysed cells by ammonium sulfate precipitation, followed by chromatography on DEAE columns (GE Healthcare Biosciences) and G50 (GE Healthcare Biosciences). Typically, 10 mg of protein was obtained from 250 mL of medium.

Site-specific labeling of proteins with 4MTDA: The ligation experiment was performed with uniformly ^{15}N labeled human ubiquitin A28C and T22C mutants. Similar to the previous ligation protocol,[12] the target protein at 0.5 mM was first activated with a fivefold excess of Ellman's reagent [5,5′-dithiobis(2-nitrobenzoic acid) (DTNB)] at pH 7.2. Excess DTNB and produced 2-nibrobenzate (TNB) were removed with a pD10 column (GE), and then eight equivalents of 4MTDA were added to the activated protein–TNB solution and the pH was adjusted to 7.4. The resultant solution was incubated at room temperature for 6 h. The 4MDTA-tagged protein sample was purified with a PD10 column, and the ligation yield was about 50–70%.

NMR spectra: NMR experiments were performed at 298 K on a Bruker AV600 NMR spectrometer equipped with a QCI cryoprobe. All ^{15}N HSQC spectra in the presence of diamagnetic or paramagnetic metal ions were recorded on 0.10 mM protein in 20 mM MES at pH 6.4 unless described otherwise. Paramagnetic or diamagnetic protein samples was prepared by titrating lanthanide ions (10 mM in stock solution) into the solution of 0.10 mM protein. PCSs were calculated from ^{15}N HSQC spectra as differences in ^1H chemical shifts between samples with paramagnetic lanthanides and diamagnetic Y^{3+}.

Calculation of the $\Delta\chi$ tensors: The $\Delta\chi$-tensor parameters were determined using the Numbat program.[24] Only PCS data from residues located in regions of well-defined secondary structure were included in the fits to the crystal structure of ubiquitin (pdb code: 1ubi).[25] Q factors were calculated by using Equation (3).[26]

$$Q = \frac{\sqrt{\sum (\mathrm{PCS}^{\mathrm{exp}} - \mathrm{PCS}^{\mathrm{cal}})^2}}{\sqrt{\sum (\mathrm{PCS}^{\mathrm{exp}})^2}} \quad (3)$$

No data from the flexible loops and the flexible C-terminal residues were used in simulations of $\Delta\chi$ tensors.

RDC measurements and calculation of alignment tensors: Residual dipolar couplings $^1D_{NH}$ were measurement as the ^{15}N-doublet splitting of the diamagnetic sample minus that of the paramagnetic sample by using the IPAP pulse sequence.[27] Alignment tensors were determined by using Module.[28] Only RDCs of residues in regular secondary-structure elements were used in fitting to the crystal structure of ubiquitin (pdb code: 1ubi),[25] and Q factors were calculated by using Equation (4).[29]

$$Q = \frac{\sqrt{\sum (\mathrm{RDC}^{\mathrm{exp}} - \mathrm{RDC}^{\mathrm{calc}})^2}}{\sqrt{\sum (\mathrm{RDC}^{\mathrm{exp}})^2}} \quad (4)$$

Acknowledgements

Financial support by 973 program (2013CB910200) and National Science Foundation of China (21073101, 21273121, and 21121002) is greatly acknowledged. We thank Dr. Thomas Huber at Research School of Chemistry in Australian National University for discussion.

[1] a) I. Bertini, C. Luchinat, G. Parigi, *Prog. Nucl. Magn. Reson. Spectrosc.* **2002**, *40*, 249–273; b) G. Otting, *J. Biomol. NMR* **2008**, *42*, 1–9; c) G.M. Clore, J. Iwahara, *Chem. Rev.* **2009**, *109*, 4108–4139; d) I. Bertini, C. Luchinat, G. Parigi, *Coord. Chem. Rev.* **2011**, *255*, 649–663; e) K. N. Allen, B. Imperiali, *Curr. Opin. Chem. Biol.* **2010**, *14*, 247–254.

[2] a) F. Rodriguez-Castañeda, P. Haberz, A. Leonov, C. Griesinger, *Magn. Reson. Chem.* **2006**, *44*, S10–S16; b) X. C. Su, G. Otting, *J. Biomol. NMR* **2010**, *46*, 101–112; c) J. Koehler, J. Meiler, *Prog. Nucl. Magn. Reson. Spectrosc.* **2011**, *59*, 360–389; d) D. Shishmarev, G. Otting, *J. Biomol. NMR* **2013**, *56*, 203–216.

[3] a) X. C. Su, K. McAndrew, T. Huber, G. Otting, *J. Am. Chem. Soc.* **2008**, *130*, 1681–1687; b) P. H. Keizers, A. Saragliadis, Y. Hiruma, M. Overhand, M. Ubbink, *J. Am. Chem. Soc.* **2008**, *130*, 14802–1481; c) D. Häussinger, J. R. Huang, S. Grzesiek, *J. Am. Chem. Soc.* **2009**, *131*, 14761–14767; d) B. Graham, C. T. Loh, J. D. Swarbrick, P. Ung, J. Shin, H. Yagi, X. Jia, S. Chhabra, N. Barlow, G. Pintacuda, T. Huber, G. Otting, *Bioconjugate Chem.* **2011**, *22*, 2118–2125; e) F. Peters, M. Maestre-Martinez, A. Leonov, L. Kovačič, S. Beckers, R. Boelens, C. Griesinger, *J. Biomol. NMR* **2011**, *51*, 329–337; f) C. T. Loh, K. Ozawa, K. L. Tuck, N. Barlow, T. Huber, G. Otting, B. Graham, *Bioconjugate Chem.* **2013**, *24*, 260–268; g) L. J. Martin, M. J. Hähnke, M. Nitz, J. Wöhnert, N. R. Silvaggi, K. N. Allen, H. Schwalbe, B. Imperiali, *J. Am. Chem. Soc.* **2007**, *129*, 7106–7113; h) K. Barthelmes, A.M. Reynolds, E. Peisach, H. R. Jonker, N. J. DeNunzio, K. N. Allen, B. Imperiali, H. Schwalbe, *J. Am. Chem. Soc.* **2011**, *133*, 808–819.

[4] a) T. Saio, K. Ogura, M. Yokochi, Y. Kobashigawa, F. Inagaki, *J. Biomol. NMR* **2009**, *44*, 157–166; b) J. D. Swarbrick, P. Ung, X. C. Su, A. Maleckis, S. Chhabra, T. Huber, G. Otting, B. Graham, *Chem. Commun.* **2011**, *47*, 7368–7370.

[5] a) X. C. Su, B. Man, S. Beeren, H. Liang, S. Simonsen, C. Schmitz, T. Huber, B. A. Messerle, G. Otting, *J. Am. Chem. Soc.* **2008**, *130*, 10486–10487; b) B. Man, X. C. Su, H. Liang, S. Simonsen, T. Huber, B. A. Messerle, G. Otting, *Chem. Eur. J.* **2010**, *16*, 3827–3832; c) X. Jia, A. Maleckis, T. Huber, G. Otting, *Chem. Eur. J.* **2011**, *17*, 6830–6836.

[6] N. L. Fawzi, M. R. Fleissner, N. J. Anthis, T. Kálai, K. Hideg, W. L. Hubbell, G.M. Clore, *J. Biomol. NMR* **2011**, *51*, 105–114.

[7] a) D. Parker, R. S. Dickins, H. Puschmann, C. Crossland, J. A. K. Howard, *Chem. Rev.* **2002**, *102*, 1977–2010; b) E. Pidcock, G. R. Moore, *J. Biol. Inorg. Chem.* **2001**, *6*, 479–489.

[8] a) J.-C. G. Bünzl, *Chem. Rev.* **2010**, *110*, 2729–2755; b) P. R. Selvin, *Methods Enzymol.* **1995**, *246*, 300–334.

[9] a) D. J. Posson, *Neuron* **2008**, *59*, 98–109; b) R. B. Best, K. A. Merchant, I. V. Gopich, B. Schuler, B. A. Bax, *Proc. Natl. Acad. Sci. USA* **2007**, *104*, 18964–18967; c) J. W. Taraska, M. C. Puljung, N. B. Olivier, G. E, W. N. Zagotta, *Nat. Methods* **2009**, *6*, 532–537.

[10] A. Wild, A. Winter, F. Schlültter, U. S. Schubert, *Chem. Soc. Rev.* **2011**, *40*, 1459–1511.

[11] a) A. K. Saha, K. Cross, E. D. Kloszewski, D. A. Upson, J. L. Toner, R. A. Snow, C. D. V. Black, V. C. Desai, *J. Am. Chem. Soc.* **1993**, *115*, 11032–11033; b) A. P. de Silva, H. Q. N. Gunaratne, T. E. Rice, *Angew. Chem.* **1996**, *108*, 2253–2255; *Angew. Chem. Int. Ed. Engl.* **1996**, *35*, 2116–2118; c) S. Poupart, C. Boudou, P. Peixoto, M. Massonneau, P.-Y. Renard, A. Romieu, *Org. Biomol. Chem.* **2006**, *4*, 4165–4177; d) M. Latva, H. Takalo, V.-M. Mukkala, C. Matachescu, J.-C. Rodriguez-Ubis, J. Kankare, *J. Lumin.* **1997**, *75*, 149–169; e) X. Y. Chen, Y. Bretonniere, J. Pecaut, D. Imbert, J. C. Bunzli, M. Mazzanti, *Inorg. Chem.* **2007**, *46*, 625–637; f) E. S. Andreiadis, R. Demadrille, D. Imbert, J. Pecaut, M. Mazzanti, *Chem. Eur. J.* **2009**, *15*, 9458–9476.

[12] X. C. Su, T. Huber, N. E. Dixon, G. Otting, *ChemBioChem* **2006**, *7*, 1599.

[13] P. Kadjane, C. Plates-Iglesias, R. Ziessel, L. J. Charbonniere, *J. Chem. Soc. Dalton Trans.* **2009**, 5688–5700.

[14] A. A. Avetisyan, I. L. Aleksanyan, L. P. Ambartsumyan, *Russ. J. Org. Chem.* **2005**, *41*, 769–771.

[15] Z. Wei, Y. Yang, Q. F. Li, F. Huang, H. H. Zuo, X. C. Su, *Chem. Eur. J.* **2013**, *19*, 5758–5764.

[16] I. Grenthe, *J. Am. Chem. Soc.* **1960**, *82*, 6258.

[17] H. Yagi, A. Maleckis, G. Otting, *J. Biomol. NMR* **2013**, *55*, 157–166.

[18] M. Assfalg, I. Bertini, P. Turano, A. G. Mauk, J. R. Winkler, H. B. Gray, *Biophys. J.* **2003**, *84*, 3917–3923.

[19] P. R. Selvin, *Ann. Rev. Biophys. Biolmol. Struct.* **2002**, *31*, 275–302.

[20] a) J. C. G. Bünzli, *Chem. Rev.* **2010**, *110*, 2729–2755; b) S. Pandya, J. Yu, D. Parker, *Dalton Trans.* **2006**, 2757–2766; c) I. Hemmilä, V. Laitala, *J. Fluoresc.* **2005**, *15*, 529–542.

[21] a) M. Kawaguchi, T. Okabe, T. Terai, K. Hanaoka, H. Kojima, I. Minegishi, T. Nagano, *Chem. Eur. J.* **2010**, *16*, 13479; b) K. Hashino, K. Ikawa, M. Ito, C. Hosoya, T. Nishioka, M. Makiuchi, K. Matsumoto, *Anal. Biochem.* **2007**, *364*, 89–91; c) V. Laitala, I. Hemmilä, *Anal. Chem.* **2005**, *77*, 1483–1487.

[22] a) I. Bertini, C. Luchinat, M. Nagulapalli, G. Parigi, E. Ravera, *Phys. Chem. Chem. Phys.* **2012**, *14*, 9149–9156; b) T. Saio, K. Ogura, K. Shimizu, M. Yokochi, T. R., Jr. Burke, F. Inagaki, *J. Biomol. NMR* **2011**, *51*, 395–408; c) C. Schmitz, R. Vernon, G. Otting, D. Baker, T. Huber, *J. Mol. Biol.* **2012**, *416*, 668–677; d) H. Yagi, K. B. Pilla, A. Maleckis, B. Graham, T. Huber, G. Otting, *Structure* **2013**, *21*, 883–890.

[23] a) H. Yagi, D. Banerjee, B. Graham, T. Huber, D. Goldfarb, G. Otting, *J. Am. Chem. Soc.* **2011**, *133*, 10418–10421; b) A. Potapov, Y. Song, T. J. Meade, D. Goldfarb, A. V. Astashkin, A. Raitsimring, *J. Magn. Reson.* **2010**, *205*, 38–49.

[24] C. Schmitz, M. J. Stanton-Cook, X. C. Su, G. Otting, T. Huber, *J. Biomol. NMR* **2008**, *41*, 179–189.

[25] R. Ramage, J. Green, T. W. Muir, O.M. Ogunjobi, S. Love, K. Shaw, *Biochem. J.* **1994**, *299*, 151–158.

[26] I. Bertini, M. B. L. Janik, Y.M. Lee, C. Luchinat, A. Rosato, *J. Am. Chem. Soc.* **2001**, *123*, 4181–4188.

[27] M. Ottiger, F. Delaglio, A. Bax, *J. Magn. Reson.* **1998**, *131*, 373–378.

[28] P. Dosset, J.-C. Hus, D. Marion, M. Blackledge, *J. Biomol. NMR* **2001**, *20*, 223–231.

[29] A. Bax, G. Kontaxis, N. Tjandra, *Methods Enzymol.* **2001**, *339*, 127–174.

Received: June 15, 2013
Published online: November 7, 2013

